Abstract

Secretory leukocyte protease inhibitor (SLPI) is a serine protease inhibitor and its expression level is positively correlated with tumor aggressiveness and metastatic potential. However, the mechanism underlying SLPI-induced enhancement of malignant phenotype is not completely understood. Malignancy of cancer cells is highly dependent on their migration activity. Previous studies revealed that gingival carcinoma Ca9-22 cells, but not colorectal adenocarcinoma HT-29 cells expressed SLPI. Therefore, the migration activity of these two cell types was investigated to understand the SLPI-mediated tumor aggressiveness and metastatic potential. *In vitro* wound healing assay indicated that HT-29 and *SLPI*-deleted Ca9-22 cells showed lower migration activity than wild type Ca9-22 cells, suggesting that SLPI-induced cell migration plays an important role in tumor aggressiveness and metastatic potential. In addition, gene expression profiling based on microarray data of the three cell types identified candidates, including LCP1, as key molecules in the mechanism of SLPI-induced cell migration.

Introductions

Secretory leukocyte protease inhibitor (SLPI), a serine protease inhibitor, plays an important role in the protection of the skin and mucosa (1,2). In normal tissues, SLPI is found in large quantities in fluids lining the mucosal surfaces, including those of the respiratory tract, inhibits bacterial infection and inflammation, and promotes wound healing and epithelial proliferation independent of its anti-protease activity (3–6). Although a previous report suggested that DNase I hypersensitivity sites in the 5′ flanking region of the *SLPI* are responsible for the transcription of *SLPI* (3), little is known how *SLPI* expression is controlled. SLPI expression increases in various human cancers, including breast, lung, and ovarian cancers, colorectal carcinoma, and glioblastoma (7–9). Further, several studies have shown that SLPI expression level is positively correlated with tumor aggressiveness and metastatic potential (10,11). Devoogdt et al. (10) reported that SLPI expression was higher in highly malignant Lewis lung carcinoma (LLC) cells than in less malignant LLC cells. Moreover, forced expression of exogenous SLPI increases both the tumorigenicity and lung metastases of LLC cells (10). To date, the mechanism underlying SLPI-induced enhancement of malignant phenotype is not completely understood. Malignancy of cancer cells is highly dependent on their migration activity (12,13). Therefore, assessment of the effect of SLPI on the migration

activity of cancer cells is important to understand mechanisms underlying the malignancy of these cells. This can be determined by performing microarray-based gene expression profiling.

HT-29 is a human colorectal adenocarcinoma cell line, and Ca9-22 is a cell line derived from the carcinoma of the gingiva (14,15). These cells exhibit epithelial morphology and have been used as *in vitro* models of cancer cells in numerous cancer research projects (16,17). Furthermore, a previous study showed that Ca9-22 cells but not HT-29 cells expressed SLPI under standard culture condition (18). Therefore, microarray-based gene expression profiling of HT-29 and Ca9-22 cells was performed for high-throughput analysis and screening differentially expressed genes (DEGs). In addition, the same analysis by using *SLPI*-deleted (Δ*SLPI*) Ca9-22 cells was performed. This doctoral thesis aimed to identify candidates that play an important role in SLPI-induced cell migration by comparing the gene expression profiles of these cells.

Materials and Methods

Cells and reagents

HT-29 and Ca9-22 cells were purchased from RIKEN BRC (Ibaraki, Japan). The cells were cultured in minimal essential medium (Wako, Tokyo, Japan) supplemented with 1% penicillin–streptomycin (Wako) and 10% fetal bovine serum (Japan Bio Serum, Tokyo, Japan) at 37°C and in 5% CO_2. Δ*SLPI* Ca9-22 cells were generated as described previously (18). Briefly, the fragment containing *SLPI* was amplified by PCR using genomic DNA from wild type Ca9-22 (wtCa9-22) cells. For the SLPI-disruption construct, the neomycin resistance gene under control of the TK promoter was inserted between NdeI sites in the *SLPI*-fragment. In total, 1×10^7 Ca9-22 cells were transfected with the plasmids inserted with the SLPI-disruption construct. After transfection, cells were selected on a medium containing G418 (Sigma-Aldrich, MO, USA).

In vitro wound healing assay

The cells were seeded in 3-cm culture dishes (cell density, 5×10^4 cells/dish) and were grown to confluence. Cell monolayers were scratched with a 2-mm-wide silicon tip in the center of the dishes, and the cells were washed once with the culture medium to remove detached cells. After incubation for 0 or 24 h, the cells were fixed with 4% paraformaldehyde for 15 min and were

stained with 0.05% toluidine blue. Stained cells were imaged using GTX-890 scanner (EPSON, Nagano, Japan).

Cell counting assay

The cells were seeded in 10-cm culture dishes (cell density, 1×10^4 cells/dish) and were cultured for 2, 4, 6, 8, 10, and 12 d in the growth medium as described above. Further, the cells were trypsinized and resuspended, and the number of cells was counted using a hemocytometer under a microscope.

Analysis of DNA synthesis

DNA synthesis was analyzed using Click-iT™ EdU Flow Cytometry Assay Kits (Thermo Fisher Scientific MA, USA) according to the manufacturer's instructions. In brief, cells were treated with 10 μM 5-ethynyl-2´-deoxyuridine (EdU) for 1 h. EdU-incorporated cells were fixed with 4% paraformaldehyde for 15 min. The cells were then treated for 30 min with the click-reaction mixture containing pacific blue azide, and resuspended in 1% BSA supplemented PBS buffer. Subsequently, the cells were analyzed on a FACS Aria (BD Biosciences, NJ, USA).

Analysis of mRNA expression

Analysis of mRNA expression was performed as described previously (19). Briefly, total RNA was isolated using RNAiso Plus (Takara Bio, Shiga, Japan), according to the manufacturer's instructions. First-strand cDNA was synthesized from 1.5 μg total RNA by using SuperScript III RNase H reverse transcriptase kit (Thermo Fisher Scientific, USA). The cDNA obtained was amplified by performing real-time RT-PCR by using SYBR Premix Ex Taq II (Takara Bio) in CFX96 Real-Time System (Bio-Rad Laboratories, CA). As such, their expression levels were confirmed by real-time RT-PCR. The levels of mRNA were normalized to those of *β-actin*. Primers used for PCR are as follows: *SLPI* (5′- GAG ATG TTG TCC TGA CAC TTG TG -3′ and 5′-AGG CTT CCT CCT TGT TGG GT -3′), *LCP1* (5′- GAT CAG TGT CCG ATG AGG AAA TG -3′ and 5′- CCA GAT CAC CTG TAG CCA TC -3′), *NOX1* (5′- CTG CTT CCT GTG TGT CGC A -3′ and 5′- AGG CAG ATC ATA TAG GCC AC -3′), and *β-actin* (5′- CTT TCT ACA ATG AGC TGC GTG -3′, and 5′- ATG GCT GGG GTG TTG AAG G -3′).

Western blotting

The cells were lysed using a sample buffer (50 mM Tris-HCl, 2% SDS, 10% glycerol, and 5% 2-mercaptoethanol). Next, samples containing 10 μg proteins were separated by performing SDS-PAGE, and the separated proteins were transferred onto nitrocellulose membranes. The membranes were incubated with primary antibodies against SLPI (dilution, 1:500; DAKO Japan,

Tokyo, Japan) and β-actin (dilution, 1:500; Santa Cruz Biotechnology, CA, USA). After washing, the membranes were incubated with HRP-conjugated secondary antibodies (dilution, 1:10,000; Cell Signaling Technology, MA, USA) for 45 min. Immunoreactive bands were visualized using an enhanced chemiluminescence kit (Amersham, IL, USA).

Gene expression profiling

Gene expression profiling was performed using microarray data of HT-29, wtCa9-22, and Δ*SLPI* Ca9-22 cells. Total RNA was extracted from each cell type by using NucleoSpin RNA kit (Takara Bio). RNA quality was determined using Agilent 2100 Bioanalyzer (Agilent Technologies, CA, USA), and 50 ng total RNA from each sample was subjected to microarray analysis by using SurePrint G3 Human 8×60K Version 1.0 Array (Agilent Technologies), according to the manufacturer's instructions. Raw data are available in the NCBI GEO database (accession No.: GSE83104). Microarray data were analyzed using GeneSpring GX software (Tomy Digital Biology, Tokyo, Japan). All data obtained from the same chip were normalized to the 75th percentile of all values on that chip. DEGs were screened using the formula 2-fold change > 1 (2-fold change = log2 [normalized intensity of sample/normalized intensity of control]). Web Gene Ontology Annotation Plot (WEGO) was used for plotting gene ontology (GO) annotation results of DEGs. KEGG pathway analysis based on hypergeometric test for DEGs was performed using EMA package.

Statistical analysis

Quantifiable results are presented as mean ± standard deviation (SD) of triplicate cultures. Statistical differences between the samples were assessed using Student's *t*-test. $P < 0.05$ was considered statistically significant.

Results

SLPI expression in HT-29, wtCa9-22, and ΔSLPI Ca9-22 cells

SLPI mRNA and protein expression was examined. WtCa9-22 cells showed remarkable *SLPI* mRNA and protein expression (Fig. 1A and B). In contrast, *SLPI* mRNA expression level in HT-29 cells was much lower than that in wtCa9-22 cells. Moreover, SLPI protein expression was negligible in HT-29 cells (Fig. 1A and B). Δ*SLPI* Ca9-22 cells were generated by replacing *SLPI* with a neomycin resistance gene (18). Δ*SLPI* Ca9-22 cells were also examined by performing real-time RT-PCR and western blotting to confirm the inhibition of *SLPI* expression. Results of real-time RT-PCR and western blotting showed that *SLPI* expression was completely inhibited at both the mRNA and protein levels in Δ*SLPI* Ca9-22 cells (Fig. 1A and B).

Migration and Proliferation of HT-29, wtCa9-22, and ΔSLPI Ca9-22 cells

The migration of HT-29, wtCa9-22, and Δ*SLPI* Ca9-22 cells was examined by performing the *in vitro* wound healing assay. Results of the assay indicated that HT-29 and Δ*SLPI* Ca9-22 cells showed lower migration from the border of the original scratch zone than wtCa9-22 cells in 24-h cultures (Fig. 1C). No remarkable difference in migration level was observed between HT-29 and Δ*SLPI* Ca9-22 cells. The proliferation of HT-29, wtCa9-22, and Δ*SLPI* Ca9-22 cells was examined

(Fig. 1D). For this, the cells were cultured in culture dishes for the indicated number of days, and cell numbers were counted at each time point. The three cell types proliferated rapidly from days 6 to 10. However, the proliferation of wtCa9-22 cells was slightly higher than that of HT-29 and Δ*SLPI* Ca9-22 cells on 10 d (Fig. 1D). As DNA synthesis is essential for cell proliferation, DNA synthesis level of the cells in logarithmic growth phase was then analyzed. Although the percentages of the cells in DNA synthesis (S) phase of HT-29 and Δ*SLPI* Ca9-22 cells seemed to be slightly lower than that of wtCa9-22 cells, there was no statistical difference between them (Fig. 1E).

Summary of DEG analyses based on microarray data

Gene expression profiling was performed using microarray data of HT-29, wtCa9-22, and Δ*SLPI* Ca9-22 cells. Approximately 36,000 transcriptomes (63,000 probes) were investigated. The increase or decrease in the expression of genes in HT-29 and Δ*SLPI* Ca9-22 cells was compared with those in wtCa9-22 cells. The number of upregulated and downregulated genes in HT-29 cells was 4,344 (> 2 fold) and 4,625 (< 0.5 fold), respectively, and that in Δ*SLPI* Ca9-22 cells was 4,396 (> 2 fold) and 4,571 (< 0.5 fold), respectively (Fig. 2A). In all, 2,917 and 3,788 genes were commonly upregulated and downregulated, respectively, in both HT-29 and Δ*SLPI* Ca9-22 cells. Top 10 genes with increased or decreased mRNA expression in *ΔSLPI* Ca9-22 and HT-29 cells

were listed in Table 1 and 2, showing that 60 % of them were common between *ΔSLPI* Ca9-22 and HT-29 cells. Scatter plot analysis showed that the difference in gene expression status between HT-29 and Δ*SLPI* Ca9-22 cells was much lower than that between these two cell types and wtCa9-22 cells (Fig. 2B).

Gene expression profiling: GO and KEGG pathway analyses

GO analysis was performed with the commonly upregulated and downregulated genes in HT-29 and Δ*SLPI* Ca9-22 cells compared with those in wtCa9-22 cells. Among them, 1,941 upregulated and 2,399 downregulated genes were assigned to 49 and 50 GO terms, respectively (Fig. 3A). The dominant terms for the upregulated genes were "cell," "cell part," "cellular process," "binding," and "organelle" (Fig. 3A). The top five dominant terms for the downregulated genes were similar to those for the upregulated genes (Fig. 3A).

As the principal aim of this study was to identify candidates that play an important role in SLPI-induced cell migration, we focused on the GO term "cell migration" to understand the functions of the upregulated and downregulated genes in HT-29 and Δ*SLPI* Ca9-22 cells compared with those in wtCa9-22 cells. Color chart showing the expression levels of genes associated with "cell migration" indicated that the gene expression pattern in HT-29 and Δ*SLPI* Ca9-22 cells was different from that in wtCa9-22 cells (Fig. 3B). Particularly, mRNA expression levels of *LCP1* were

much lower in both HT-29 and Δ*SLPI* Ca9-22 cells than in wtCa9-22 cells (Fig. 3B). In contrast, mRNA levels of *NOX1* were much higher in both HT-29 and Δ*SLPI* Ca9-22 cells than in wtCa9-22 cells (Fig. 3B).

Next, DEGs that were common between HT-29 and Δ*SLPI* Ca9-22 cells compared with those in wtCa9-22 cells were examined by using the KEGG pathway database to identify the molecular interaction and reaction networks for SLPI-induced cell migration. In all, 741 upregulated genes and 921 downregulated genes were grouped into 282 and 284 KEGG pathways, respectively (Fig. 3C). The top three pathways of the upregulated and downregulated genes were metabolic pathways, cancer pathways, and PI3K–Akt signaling pathway (Fig. 3C). Interestingly, cAMP signaling pathway contained 45 downregulated genes, although no upregulated gene was associated with this pathway (Fig. 3C)

Lastly, as present GO data of "cell migration" term showed mostly difference in the mRNA expression of *LCP1* and *NOX1* between wtCa9-22 cells and the other two cell types, which was confirmed by real-time RT-PCR, and consisted with the microarray data (Fig. 4).

Discussion

This study showed that SLPI was weakly expressed in HT-29 cells compared with that in wtCa9-22 cells, and that the migration and proliferation of HT-29 and Δ*SLPI* Ca9-22 cells were lower than that of wtCa9-22 cells. These results indicate that SLPI regulats the proliferation and migration of HT-29 and wtCa9-22 cells. Both cell proliferation and migration are closely associated with tumor aggressiveness and metastatic potential (12,13). SLPI is highly expressed in various cancers, including inflammatory breast cancer, which has high angiogenic and metastatic capacities (11,21,22). Further, forced expression of exogenous SLPI in lung carcinoma cells remarkably increases their tumorigenicity and lung metastasis after subcutaneous inoculation (10). These findings suggest that SLPI promotes tumor aggressiveness and metastatic potential in part by regulating cell proliferation and migration. However, in this study, a small difference in proliferation was observed between wtCa9-22 cells and the other two cell types. Furthermore, no statistical difference in DNA synthesis level was observed between the three cell types. In contrast, the migration level of wtCa9-22 cells was completely different from that of the other two cell types. These results suggest that SLPI promoted tumor aggressiveness and metastatic potential not by regulating their proliferation but by regulating their migration. Furthermore, these results suggest

that the molecular mechanism underlying SLPI-induced cell migration was different from that of cell proliferation.

Next, the gene expression profile of wtCa9-22 cells was compared with those of the other two cell types to identify candidates that play an important role in SLPI-induced cell migration. In all, 4,344 and 4,396 genes were upregulated in HT-29 and Δ*SLPI* Ca9-22 cells, respectively, compared with those in wtCa9-22 cells. Of these, 2,917 genes were common between HT-29 and Δ*SLPI* Ca9-22 cells. Similarly, many downregulated genes (approximately 80% in each cell line) were common between HT-29 and Δ*SLPI* Ca9-22 cells. Scatter plot analysis showed that gene expression pattern was similar between HT-29 and Δ*SLPI* Ca9-22 cells compared with that between these two cell types and wtCa9-22 cells. These results suggested that lower migration level of HT-29 and Δ*SLPI* Ca9-22 cells compared with that of wtCa9-22 cells was promoted by the same molecular mechanism. Therefore, the DEGs that were common between HT-29 and Δ*SLPI* Ca9-22 cells were analyzed by performing GO and KEGG pathway analyses.

GO analysis showed that the expression pattern of genes associated with “cell migration” was similar between HT-29 and Δ*SLPI* Ca9-22 cells compared with that between these two cells types and wtCa9-22 cells, which was consistent with the results of the scatter plot analysis. Among genes associated with “cell migration,” we focused on *LCP1* and *NOX1* because their mRNA expression levels were mostly up- or downregulated in HT-29 and Δ*SLPI* Ca9-22 cells as compared to those in

wtCa9-22 cells. Nox1 is a catalytic subunit of the superoxide-generating NADPH oxidase in phagocytes (23,24). Previously it had been reported that Nox1 contributes to cell migration (23). For example, Nox1-dependent superoxide production enhanced colon adenocarcinoma migration (23). In contrast to the previous reports, *Nox1* mRNA expression was downregulated in HT-29 and *ΔSLPI* Ca9-22 cells as compared to that in wtCa9-22 cells, although migration level of the former was lower than that of the later. Thus, Nox1 may not be a key molecule for SLPI-induced migration in wtCa9-22 cells.

In contrast, *LCP1* was abundantly expressed in wtCa9-22 cells but was scarcely expressed in both HT-29 and Δ*SLPI* Ca9-22 cells, which was confirmed by real-time RT-PCR. LCP1 belongs to a family of actin-binding proteins that are expressed in most tissues of higher eukaryotes (25). In normal conditions, LCP1 is mainly expressed by cells of the hematopoietic lineage (25); however, in pathological conditions, it is expressed in various malignant human cells of non-hematopoietic origin, and enhances migration and metastasis of cancer cells (25, 26). A previous study showed that glioma-associated oncogene family zinc finger (GLI), a zinc finger transcription factor, upregulated LCP1 expression in human breast cancer cells (26) (Fig. 5). GLI activity is regulated by its phosphorylation through cAMP signaling pathway and is thought to be crucial for the development and progression of various human cancers, including lung, pancreatic, prostate, and breast cancers (26–28). In addition, our results of KEGG analysis showed that 45 downregulated genes were

associated with “cAMP signaling pathway,” whereas no upregulated gene was associated with this pathway, suggesting the inactivated status of the cAMP signaling pathway in HT-29 and Δ*SLPI* Ca9-22 cells. Together, these results suggest that SLPI enhances LCP1 expression by upregulating GLI activity through cAMP signaling pathway, which results in the SLPI-induced cell migration (Fig. 5).

Conclusions

The present results indicated that SLPI plays an important role in the migration of cancer cells, suggesting that it may be crucial for tumor aggressiveness and metastatic potential. In addition, the present results suggest that LCP1 and GLI might be the key molecules involved in SLPI-induced cell migration. Taken together, the results will provide a substantial transcriptome-level resource for the study of cell migration and further help the understanding of molecular mechanisms underlying the malignancy of cancer cells.

Acknowledgements

I am grateful to Profs. Hiderou Ohki, Kazuo Komiyama and Assoc. Prof. Yoshikazu Mikami (Division of Microscopic Anatomy, Niigata University Graduate School of Medical and Dental Sciences) for their valuable suggestions.

References

1. Thompson RC, Ohlsson K (1986) Isolation, properties, and complete amino acid sequence of human secretory leukocyte protease inhibitor, a potent inhibitor of leukocyte elastase. Proc Natl Acad Sci USA 83, 6692–6696.
2. Franken C, Meijer CJ, Dijkman JH (1989) Tissue distribution of antileukoprotease and lysozyme in humans. J Histochem Cytochem 37, 493–498.
3. Abe T, Kobayashi V, Yoshimura K, Trapnell BC, Kim H, Hubbard RC, et al. (1991) Expression of the secretory leukoprotease inhibitor gene in epithelial cells. J Clin Invest 87, 2207–2215.
4. Song XY, Zeng L, Jin W, Thompson J, Mizel DE, Lei K, et al. (1999) Secretory leukocyte protease inhibitor suppresses the inflammation and joint damage of bacterial cell wall-induced arthritis. J Exp Med 190, 535–542.
5. Zhu J, Nathan C, Jin W, Sim D, Ashcroft GS, Wahl SM, et al. (2002) Conversion of proepithelin to epithelins: roles of SLPI and elastase in host defense and wound repair. Cell 111, 867–878.
6. Zhang D, Simmen RC, Michel FJ, Zhao G, Vale-Cruz D, Simmen FA (2002) Secretory leukocyte protease inhibitor mediates proliferation of human endometrial epithelial cells by positive and negative regulation of growth-associated genes. J Biol Chem 277, 29999–30009.

7. Barker SD, Coolidge CJ, Kanerva A, Hakkarainen T, Yamamoto M, Liu B et al. (2003) The secretory leukoprotease inhibitor (SLPI) promoter for ovarian cancer gene therapy. J Gene Med 5, 300–310.

8. Ameshima S, Ishizaki T, Demura Y, Imamura Y, Miyamori I, Mitsuhashi H (2000) Increased secretory leukoprotease inhibitor in patients with nonsmall cell lung carcinoma. Cancer 89, 1448–1456.

9. Koshikawa N, Nakamura T, Tsuchiya N, Isaji M, Yasumitsu H, Umeda M, et al. (1996) Purification and identification of a novel and four known serine proteinase inhibitors secreted by human glioblastoma cells. J Biochem 119, 334–339.

10. Devoogdt N, Hassanzadeh G, hassabeh G, Zhang J, Brys L, De Baetselier P, et al. (2003) Secretory leukocyte protease inhibitor promotes the tumorigenic and metastatic potential of cancer cells. Proc Natl Acad Sci USA 100, 5778–5782.

11. Kluger HM, Chelouche LD, Kluger Y, McCarthy MM, Kiriakova G, Camp RL, et al. (2005) Using a xenograft model of human breast cancer metastasis to find genes associated with clinically aggressive disease. Cancer Res 65, 5578–5587.

12. Chou RH, Wen HC, Liang WG, Lin SC, Yuan HW, Wu CW, et al. (2012) Suppression of the invasion and migration of cancer cells by SERPINB family genes and their derived peptides. Oncol Rep 27, 238–245.

13. Zhang Y, Liu S, Wang H, Yang W, Li F, Yang F, et al. (2015) Elevated NIBP/TRAPPC9 mediates tumorigenesis of cancer cells through NFκB signaling. Oncotarget 6, 6160–6178.

14. Fogh J, Trempe G (1975) New human tumor cell lines. In: Fogh J (ed) Human tumor cell *in vitro*, 1st edn. Springer, New York, pp 115.

15. Horikoshi M, Kimura Y, Nagura H, Ono T, Ito H (1974) A new human cell line derived from human carcinoma of the gingiva. Jpn J Oral Surg 2, 100–106.

16. Baba T, Kawaguchi M, Fukushima T, Sato Y, Orikawa H, Yorita K, et al. (2012) Loss of membrane-bound serine protease inhibitor HAI-1 induces oral squamous cell carcinoma cells' invasiveness. J Pathol 228, 181–192.

17. Horng CT, Yang JS, Chiang JH, Lu CC, Lee CF, Chiang NN, et al. (2016) Inhibitory effects of tetrandrine on epidermal growth factor-induced invasion and migration in HT29 human colorectal adenocarcinoma cells. Mol Med Rep 13, 1003–1009.

18. Mikami Y, Iwase T, Komiyama Y, Matsumoto N, Oki H, Komiyama K (2015) Secretory leukocyte protease inhibitor inhibits expression of polymeric immunoglobulin receptor via the NF-κB signaling pathway. Mol Immunol 67, 568–574.

19. Mikami Y, Yamamoto Y, Akiyama Y, Kobayashi M, Watanabe E, Watanabe N, et al. (2015) Osteogenic gene transcription is regulated via gap junction-mediated cell-cell communication. Stem Cells 24, 214–227.

20. Bertucci F, Finetti P, Rougemont J, Charafe-Jauffret E, Nasser V, Loriod B, et al. (2004) Gene expression profiling for molecular characterization of inflammatory breast cancer and prediction of response to chemotherapy. Cancer Res 64, 8558–8565.

21. Wang G, Lim DS, Choi BD, Park JJ, Jeong SJ, Kim JS, et al. (2011) Effect of secretory leukocyte protease inhibitor on migration and invasion of human KB oral carcinoma cells. Anim Cells Syst 15, 139–146.

22. Devoogdt N, Revets H, Ghassabeh GH, De Baetselier P (2004) Secretory leukocyte protease inhibitor in cancer development, Ann NY Acad Sci 1028, 380–389.

23. Sadok A, Bourgarel-Rey V, Gattacceca F, Penel C, Lehmann M, Kovacic H (2008) Nox1-dependent superoxide production controls colon adenocarcinoma cell migration. Biochim Biophys Acta 1783, 23–33

24. Reddy MM, Fernandes MS, Salgia R, Levine RL, Griffin JD, Sattler M (2011) NADPH oxidases regulate cell growth and migration in myeloid cells transformed by oncogenic tyrosine kinases. Leukemia 25, 281–289.

25. Riplinger SM, Wabnitz GH, Kirchgessner H, Jahraus B, Lasitschka F, Schulte B, et al. (2014) Metastasis of prostate cancer and melanoma cells in a preclinical in vivo mouse model is enhanced by L-plastin expression and phosphorylation. Mol Cancer 18, 13–10.

26. Inaguma S, Riku M, Ito H, Tsunoda T, Ikeda H, Kasai K (2015) GLI1 orchestrates

CXCR4/CXCR7 signaling to enhance migration and metastasis of breast cancer cells. Oncotarget 6, 33648–33657.

27. Asaoka Y (2012) Phosphorylation of Gli by cAMP-dependent protein kinase. Vitam Horm 88, 293–307.

28. Luongo C, Ambrosio R, Salzano S, Dlugosz AA, Missero C, Dentice M (2014) The sonic hedgehog-induced type 3 deiodinase facilitates tumorigenesis of basal cell carcinoma by reducing Gli2 inactivation. Endocrinology 155, 2077–2088.

Table 1. Top 10 upregulated and downregulated genes in *ΔSLPI* Ca9-22 compared to wtCa9-22 cells

Upregulated genes in *ΔSLPI* Ca9-22 cells		
Gene symbol	**Description**	**Fold change**
SPINK1	serine peptidase inhibitor, Kazal type 1	11607.1
S100P	S100 calcium binding protein P	1965.0
EMC10	ER membrane protein complex subunit 10	1577.9
TESC	tescalcin	1464.7
ABCC3	ATP-binding cassette, sub-family C member 3	1274.3
NPDC1	neural proliferation, differentiation and control, 1	865.9
CLDN3	claudin 3	836.5
HSD17B2	hydroxysteroid dehydrogenase 2	819.6
HTATIP2	HIV-1 Tat interactive protein 2	780.0
FBP1	fructose-1,6-bisphosphatase 1	777.6
Downregulated genes in *ΔSLPI* Ca9-22 cells		
Gene symbol	**Description**	**Fold change**
ANXA8L1	annexin A8-like 1	0.00006
MIR205HG	MIR205 host gene	0.00016
ACKR3	atypical chemokine receptor 3	0.00020
BASP1	brain abundant, membrane attached signal protein 1	0.00027
HIST1H1A	histone cluster 1	0.00069
CAV1	caveolin 1	0.00103
EFEMP1	EGF containing fibulin-like extracellular matrix protein 1	0.00126
ADIRF	adipogenesis regulatory factor	0.00143
BMP7	bone morphogenetic protein 7	0.00163
PTPRU	protein tyrosine phosphatase, receptor type, U	0.00167

Table 2. Top 10 upregulated and downregulated genes in HT-29 cells compared to wtCa9-22 cells

Upregulated genes in HT-29 cells		
Gene symbol	**Description**	**Fold change**
SPINK1	serine peptidase inhibitor, Kazal type 1	10826.0
S100P	S100 calcium binding protein P	2143.2
PHGR1	proline/histidine/glycine-rich 1	1485.8
TESC	tescalcin	1130.1
ABCC3	ATP-binding cassette, sub-family C member 3	1049.0
EMC10	ER membrane protein complex subunit 10	1025.7
HSD17B2	hydroxysteroid (17-beta) dehydrogenase 2	912.5
NPDC1	r neural proliferation, differentiation and control 1	897.4
CLDN3	claudin 3	830.6
HPDL	4-hydroxyphenylpyruvate dioxygenase-like	667.0
	Downregulated genes in HT-29 cells	
Gene symbol	**Description**	**Fold change**
MIR205HG	MIR205 host gene	0.00019
ANXA8L1	annexin A8-like 1	0.00029
ADIRF	adipogenesis regulatory factor	0.00047
BASP1	brain abundant, membrane attached signal protein 1	0.00054
KRT6C	keratin 6C	0.00071
WDR66	WD repeat domain 66	0.00125
COL5A1	collagen, type V, alpha 1	0.00138
LMO1	LIM domain only 1	0.00140
EFS	embryonal Fyn-associated substrate	0.00143
CALD1	caldesmon 1	0.00171

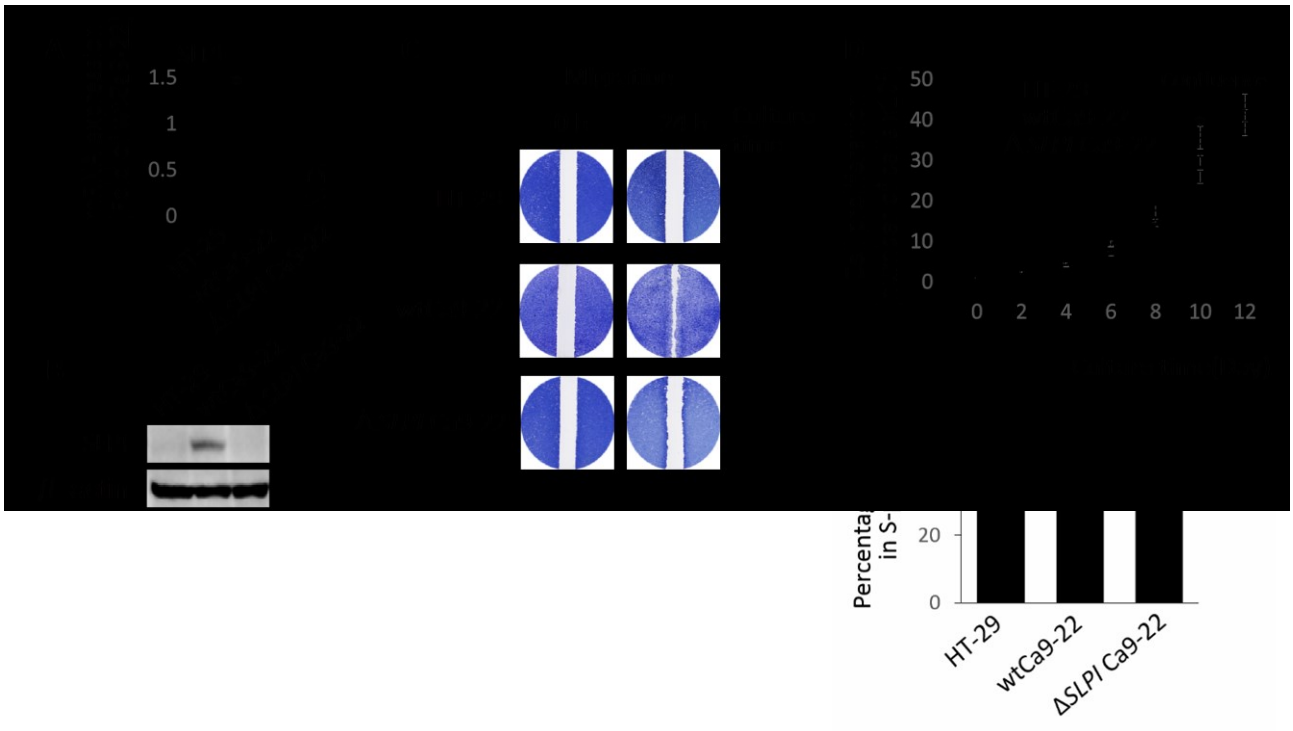

Fig. 1. Cell proliferation and migration in three cell types

(A) *SLPI* mRNA expression. RNA isolated from cells in the logarithmic growth phase was used for performing real-time RT-PCR analysis. Data are expressed as mean ± SD (n = 3, $P < 0.05$). *Significantly different from that in wtCa9-22 cells; N.D., not detected. (B) SLPI protein expression. Lysates of cells in the logarithmic growth phase were used for Western blot analysis. β-actin was used as the loading control. (C) Cell migration. A scratch (wound) was made using a silicone tip at the center of a confluent monolayer culture, and the cells were cultured further for the indicated time. Further, cell layers were fixed and stained with toluidine blue. (D) Cell proliferation. Cells were cultured in the growth medium for the indicated number of days, and cell numbers were counted. Data are expressed as mean ± SD (n = 3, $P < 0.05$). The cultures reached confluence in 12 d. *Significantly different from that in wtCa9-22 cells at each time point. (E) DNA synthesis. Cells in logarithmic growth phase were treated with EdU for 1 h. EdU-incorporated cells were labeled by pacific blue azide and detected by FACS analysis using 407 nm excitation with a 450/50 nm bandpass filter. Data are expressed as mean ± SD (n = 3, $P < 0.05$)

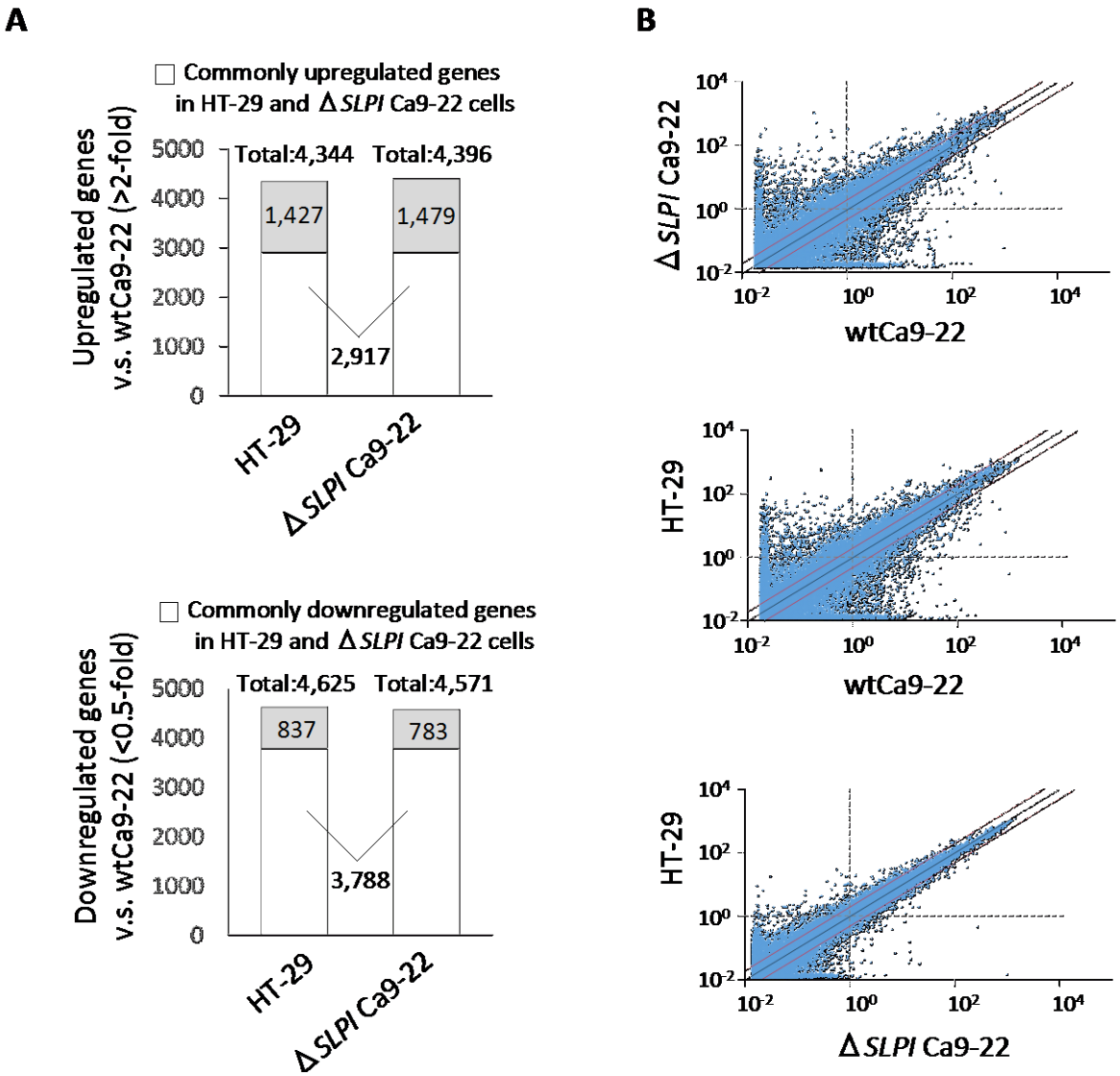

Fig. 2. Summary of DEG analyses based on microarray data

(A) The numbers of DEGs in HT-29 and Δ*SLPI* Ca9-22 cells compared with those in wtCa9-22 cells. The numbers of DEGs were counted based on microarray data. (B) Scatter plot analysis showing the expression levels of DEGs against the background of all transcripts for the indicated cell types on the x-axis and y-axis.

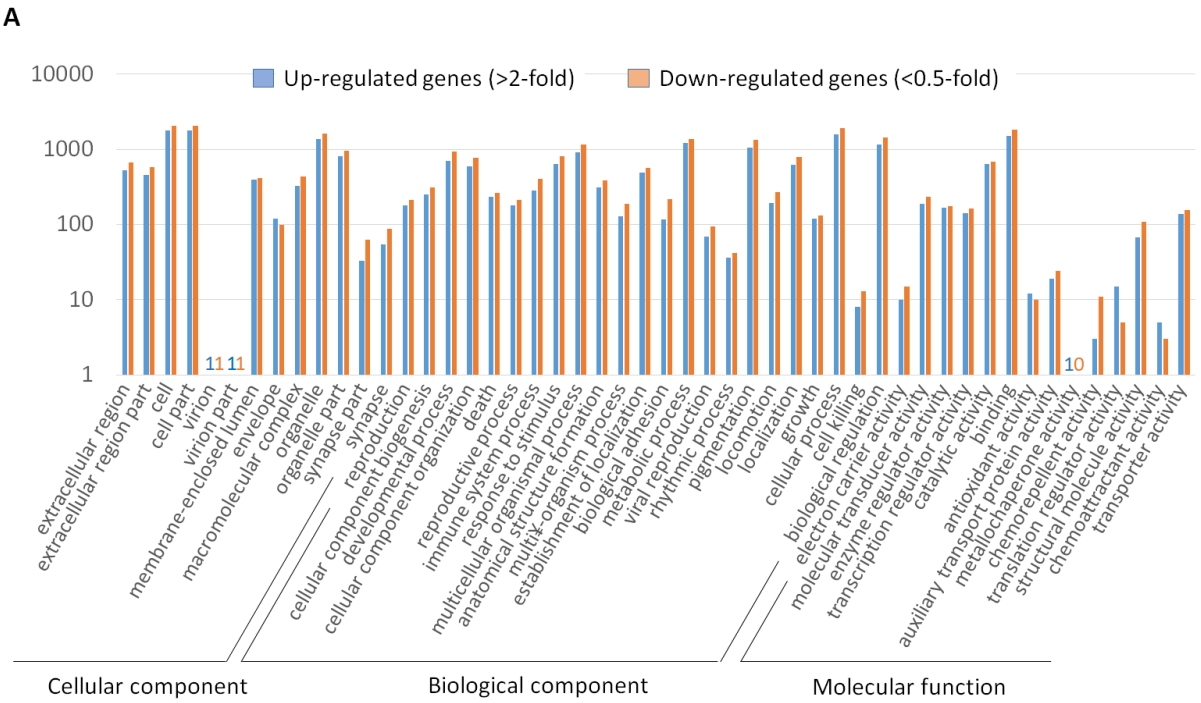
A
Up-regulated genes (>2-fold)
Down-regulated genes (<0.5-fold)
10000
1000
100
10
1
11 11
10
extracellular region
extracellular region part
cell
cell part
virion
virion part
membrane-enclosed lumen
envelope
macromolecular complex
organelle
organelle part
synapse
synapse part
reproduction
cellular component biogenesis
developmental process
cellular component organization
death
reproductive process
immune system process
response to stimulus
multicellular organismal process
anatomical structure formation
multi-organism process
establishment of localization
biological adhesion
metabolic process
viral reproduction
rhythmic process
pigmentation
locomotion
localization
growth
cellular process
cell killing
biological regulation
electron carrier activity
molecular transducer activity
enzyme regulator activity
transcription regulator activity
catalytic activity
binding
antioxidant activity
auxiliary transport protein activity
metallochaperone activity
chemorepellent activity
translation regulator activity
structural molecule activity
chemoattractant activity
transporter activity
Cellular component
Biological component
Molecular function

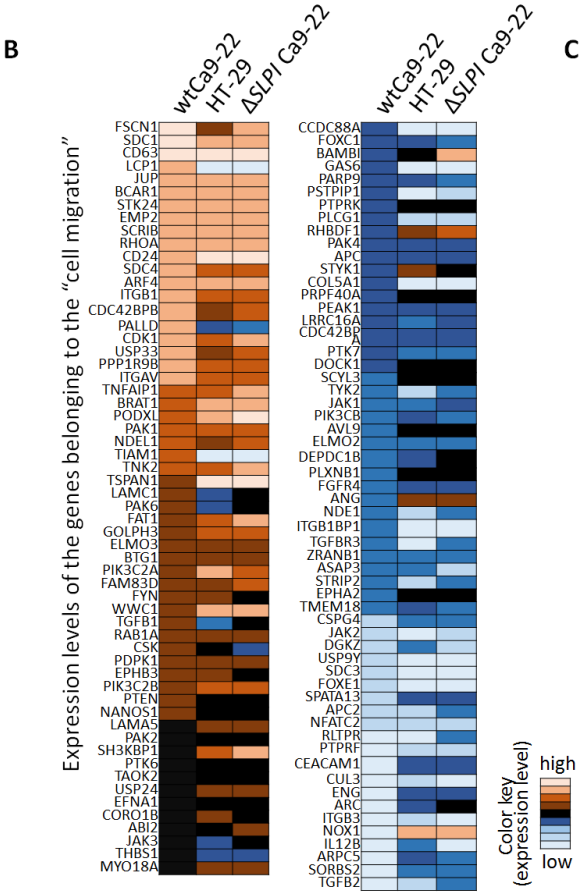
B
wtCa9-22
HT-29
ΔSLPI Ca9-22
wtCa9-22
HT-29
ΔSLPI Ca9-22
Expression levels of the genes belonging to the "cell migration"
FSCN1
SDC1
CD63
LCP1
JUP
BCAR1
STK24
EMP2
SCRIB
RHOA
CD24
SDC4
ARF4
ITGB1
CDC42BPB
PALLD
CDK1
USP33
PPP1R9B
ITGAV
TNFAIP1
BRAT1
PODXL
PAK1
NDEL1
TIAM1
TNK2
TSPAN1
LAMC1
PAK6
FAT1
GOLPH3
ELMO3
BTG1
PIK3C2A
FAM83D
FYN
WWC1
TGFB1
RAB1A
CSK
PDPK1
EPHB3
PIK3C2B
PTEN
NANOS1
LAMA5
PAK2
SH3KBP1
PTK6
TAOK2
USP24
EFNA1
CORO1B
ABI2
JAK3
THBS1
MYO18A
CCDC88A
FOXC1
BAMBI
GAS6
PARP9
PSTPIP1
PTPRK
PLCG1
RHBDF1
PAK4
APC
STYK1
COL5A1
PRPF40A
PEAK1
LRRC16A
CDC42BPA
PTK7
DOCK1
SCYL3
TYK2
JAK1
PIK3CB
AVL9
ELMO2
DEPDC1B
PLXNB1
FGFR4
ANG
NDE1
ITGB1BP1
TGFBR3
ZRANB1
ASAP3
STRIP2
EPHA2
TMEM18
CSPG4
JAK2
DGKZ
USP9Y
SDC3
FOXE1
SPATA13
APC2
NFATC2
RLTPR
PTPRF
CEACAM1
CUL3
ENG
ARC
ITGB3
NOX1
IL12B
ARPC5
SORBS2
TGFB2
Color key (expression level)
high
low
C
Up-regulated genes (>2-fold)
Metabolic pathways
Pathways in cancer
PI3K-Akt signaling pathway
Neuroactive ligand-receptor interaction
MAPK signaling pathway
Transcriptional misregulation in cancer
Cytokine-cytokine receptor interaction
Endocytosis
Ras signaling pathway
Regulation of actin cytoskeleton
0
50
100
150
200
Down-regulated (<0.5-fold)
Metabolic pathways
Pathways in cancer
PI3K-Akt signaling pathway
Focal adhesion
HTLV-I infection
Rap1 signaling pathway
Proteoglycans
MAPK signaling pathway
Ras signaling pathway
cAMP signaling pathway
0
50
100
150

Fig. 3. Gene expression profiling: GO and KEGG pathway analyses

(A) GO assignments. Common DEGs between HT-29 and Δ*SLPI* Ca9-22 cells were analyzed. Results are summarized in three main categories, cellular component, biological process, and molecular function. Classified gene objects are depicted as absolute numbers of the total number of gene objects with GO assignments. (B) Expression levels of genes associated with the GO term "cell migration." A light red region in the heat map indicates high expression, and a light blue region indicates low expression. Black indicates medial expression. (C) Pathway enrichment analysis. Common upregulated and downregulated genes between HT-29 and Δ*SLPI* Ca9-22 cells were grouped into the KEGG pathways.

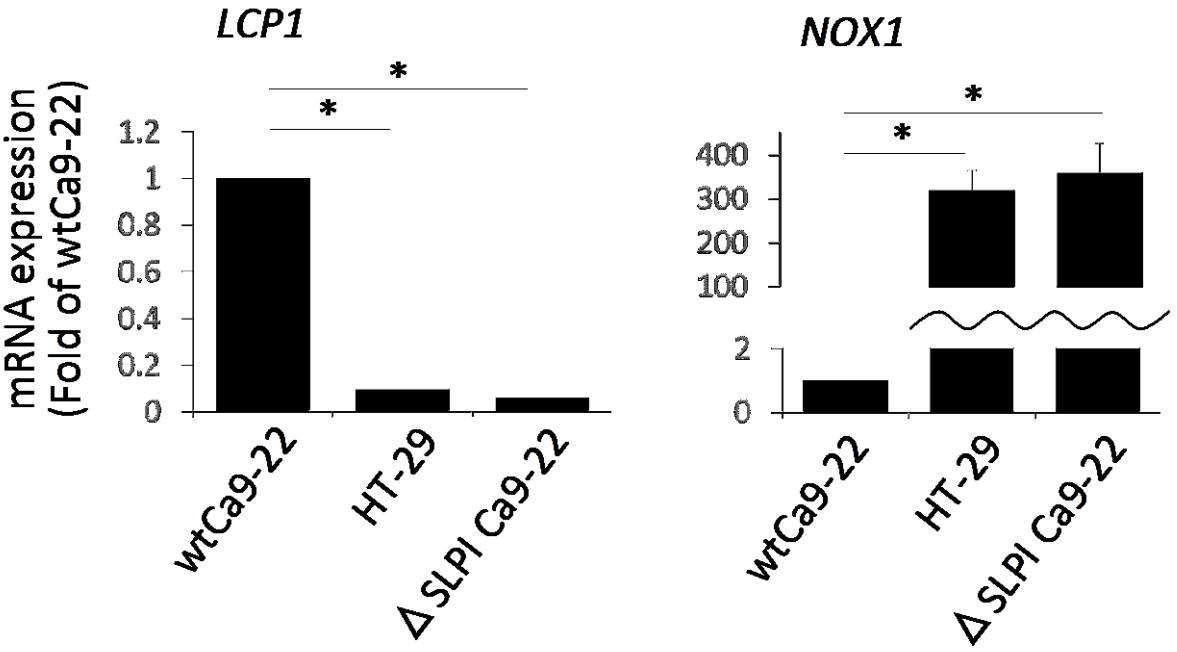

Fig. 4. mRNA expression of LCP1 and NOX1 in wtCa9-22, HT-29, and ΔSLPI Ca9-22 cells

RNA isolated from cells in the logarithmic growth phase was used for performing real-time RT-PCR. Data are expressed as mean ± SD (n = 3, $P < 0.05$). *Significantly different from that in wtCa9-22 cells.

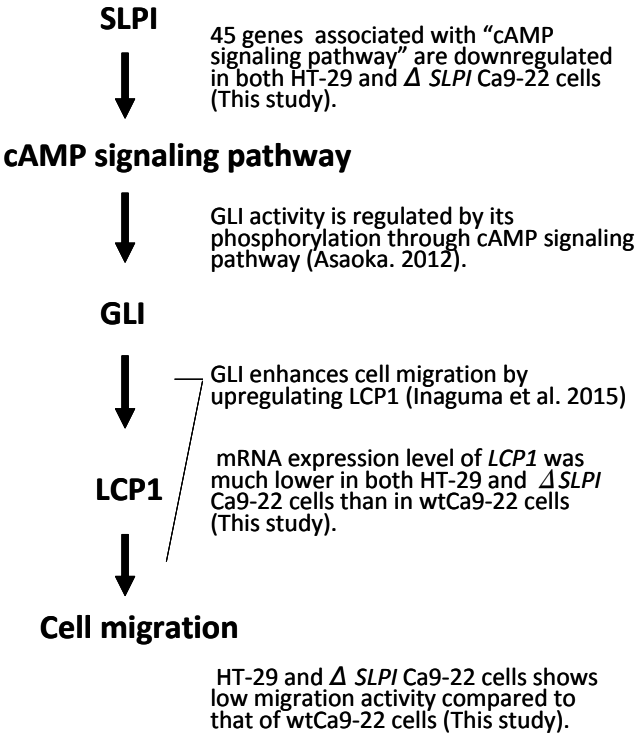

Fig. 5. A proposal model of SLPI-induced cell migration

Based on the present results and previous reports, it was suggested that SLPI induces cell migration through the indicated signaling cascade including cAMP signaling pathway, GLI and LCP1.